

## Modeling the Atmospheres of Massive Stars

Joachim Puls

Universitätssternwarte München, Scheinerstr. 1, D-81679 München, Germany

### Abstract

In this review I summarize state-of-the-art approaches to model the atmospheres of massive stars, including their line-driven winds, and provide some examples for the potential impact of stellar pulsations on such atmospheres.

Session: Atmospheres, mass loss and stellar winds

### Hot star model atmospheres

Most of our knowledge about the physical parameters of hot stars<sup>1</sup> (e.g., effective temperatures, gravities, wind-properties, chemical composition of the outer layers) originates from *quantitative spectroscopy*, i.e., the analysis of stellar spectra by means of atmospheric models.<sup>2</sup> The numerical “construction” of such atmospheric models is a tremendous challenge, mostly because of the intense radiation fields of hot stars which lead to a number of effects that are not present in the atmospheres of cooler, less massive stars. In the following, I outline the basic ingredients which have to be adequately considered to allow for a reasonable description of the outer layers of massive stars.

#### Non-local thermodynamic equilibrium (NLTE)

In addition to the intense radiation field, massive stars have rather low densities,  $\rho$ , in their line and continuum forming regions. For objects not too close to the Eddington limit, the density in (quasi-) hydrostatic regions (“photosphere”) depends almost solely on the pressure scale height,  $H$ , and the column density,  $m$ , (remember that  $m$  is roughly proportional to any reference optical depth scale,  $\tau$ )

$$\rho(m) \approx \frac{1}{H} m \propto \frac{g}{T_{\text{eff}}} m \propto \frac{M_*/M_\odot}{(R_*/R_\odot)^2 T_{\text{eff}}/T_\odot} m \quad (1)$$

(with  $g$  the gravitational acceleration), i.e., at a given  $m$  (or  $\tau$ ) the density of a typical O-dwarf with  $10 M_\odot$ ,  $10 R_\odot$  and  $T_{\text{eff}} = 30,000$  K is a factor of 50 lower than in the sun. Thus collisions are less important in hot star atmospheres, at least in the upper photosphere/wind

---

<sup>1</sup>defined here to comprise OBA-stars, Luminous Blue Variables (LBVs) and Wolf-Rayet (WR) stars, and also Central Stars of Planetary Nebulae (CSPN), which have similar atmospheres as their massive O-star counterparts.

<sup>2</sup>For stars with  $T_{\text{eff}} \gtrsim 30$  kK, photometric methods become completely unreliable discriminators of temperatures and gravities, due to the insensitivity of the Rayleigh-Jeans tail of the spectral energy distribution on temperature (e.g., Hummer et al. 1988).

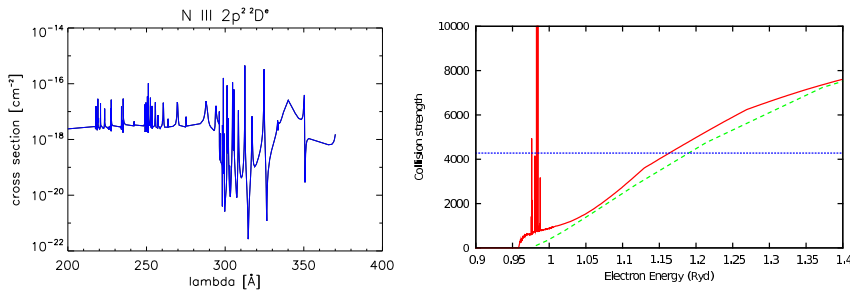


Figure 1: Examples for required atomic data. *Left*: Photo-ionization cross section of N III  $2p^2 \ 2D^o$ . Note the multitude of resonances (from Opacity Project, Seaton et al. 1992). *Right*: Comparison of collision strengths for the  $n = 4$  to  $n' = 5$  transition in hydrogen. Red (solid): Butler (2009, in preparation; see also Przybilla & Butler 2004), a 28 state close-coupling calculation; green (dashed): Percival & Richards (1978), semi-classical approximation (note that the theory should only be accurate for  $n, n' \geq 5$ ); blue (dotted): the van Regemorter (1962) approximation with  $\bar{g} = 0.2$ .

and regarding the UV/optical transitions.<sup>3</sup> In combination with the intense radiation field, this leads to the requirement that the occupation numbers of the atomic levels,  $n_i$ , have to be calculated from the NLTE rate equations (rather than from the Saha-Boltzmann equations),

$$n_i \sum_{j \neq i} (R_{ij} + C_{ij}) = \sum_{j \neq i} n_j (R_{ji} + C_{ji}), \quad (2)$$

with radiative and collisional rates  $R_{ij}$  and  $C_{ij}$ , respectively, and including all bound-bound and bound-free processes. Since the radiative rates depend on the radiation field, whereas the radiation field depends on the opacities and emissivities, which themselves are functions of the occupation numbers, the rate-equations (for all levels  $n_i$ ) have to be solved in parallel with the equations of radiative transfer (for all required frequencies). In order to prevent the stagnation of the ordinary Lambda-iteration, a delicate iteration scheme (*accelerated Lambda-iteration*) has to be implemented as well.

#### Atomic data

To calculate the radiative and collisional rates, detailed knowledge about the *individual* cross sections is required. Even though a large number of such data is available now (as calculated, e.g., within the OPAL project (Iglesias & Rogers 1996 and references therein), the *Opacity Project* (Seaton et al. 1992, for an example, see Fig. 1, left panel), and the *Iron Project* (Paper I: Hummer et al. 1993 until (to-date) Paper LXV: Witthoeft & Badnell 2008), most atmospheric codes do *not* contain the “best” data by default, but the individual user is responsible for compiling those data into appropriate *model atoms* (e.g., Przybilla & Butler 2001). Moreover, certain atoms/ions still lack a comprehensive description, particularly with respect to collisional data. An interesting example refers to the *hydrogen* bound-bound collision strengths, which have been (re-)considered in detail just recently (cf. Fig. 1, right panel), and significantly impact the strength of hydrogen IR-lines (Przybilla & Butler 2004). Finally, the number of levels and transitions in iron-group atoms is so large that certain simplifications need to be made in order to keep the problem treatable, mostly by packing several levels with close enough energies into one so-called *super-level* (Anderson 1985, 1989).

<sup>3</sup>IR-transitions depend crucially on collisional processes, due to the lower energy separation of the involved levels.

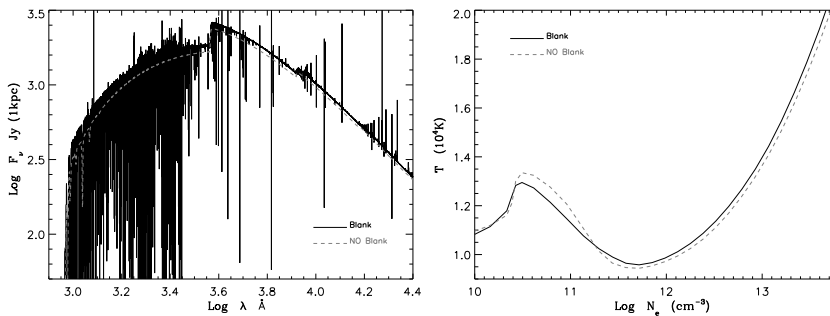


Figure 2: Effects of line blanketing (solid: blanketed model, dashed: model without blanketing) on the flux distribution ( $\log F_\nu$  (Jansky) vs.  $\log \lambda$  (Å), left panel) and temperature structure ( $T(10^4$  K) vs.  $\log n_e$ , right panel) in the atmosphere of a late B-hypergiant. Blanketing blocks flux in the UV, redistributes it towards longer wavelengths and causes back-warming. From Puls et al. (2008).

### Line-blocking/blanketing

Just as for LTE models, also NLTE models require a careful consideration of line-blocking/blanketing effects, due to the immense number of lines in the EUV. Various techniques are applied to deal with the problem, using opacity distribution functions (ODFs, suitable under LTE conditions, Kurucz 1979), opacity sampling methods (Pauldrach et al. 2001), direct line-by-line calculations (involving model atoms consisting of super-levels, Hillier & Miller 1998, Hubeny 1998), and a more approximate method based on a simple statistical approach to calculate suitable means of line opacities and emissivities (Puls 2005). An example of the corresponding effects is given in Fig. 2, with the most prominent one being the reduction of the effective temperature scale for OB-stars, summarized in this volume by F. Martins. For a detailed discussion, we refer to Repolust et al. (2004).

### Stellar winds

Due to their high luminosity, all massive stars display stellar winds, (mostly) driven by radiative line acceleration, since there are numerous spectral lines with high interaction probability close to the stellar flux maximum. Due to the acceleration mechanism, the mass-loss is metallicity dependent. Typical mass-loss rates range from  $10^{-7} M_\odot \text{yr}^{-1}$  (with even lower values for late-O and B-dwarfs) up to  $10^{-5} M_\odot \text{yr}^{-1}$  (WR-stars and LBVs), and terminal velocities scale with the photospheric escape velocity, from  $200 \text{ km s}^{-1}$  (A-supergiants) to  $\gtrsim 2000 \text{ km s}^{-1}$  (O-stars). Pioneering investigations have been performed by Lucy & Solomon (1970) and Castor, Abbott & Klein ("CAK", 1975), and important improvements with respect to a quantitative description have been provided by Friend & Abbott (1986) and Pauldrach, Puls & Kudritzki (1986). A recent review on line-driven winds has been given by Puls, Vink & Najarro (2008; see also Kudritzki & Puls 2000).

### Unified model atmospheres

With respect to the construction of atmospheric models, a consistent treatment of photosphere and wind is required, at least if the lines/continua are formed outside the (quasi-) hydrostatic region. Such *unified* model atmospheres were introduced by Gabler et al. (1986). Fig. 3 compares the electron-density distribution, as a function of the optical depth scale, for a hydrostatic atmosphere and unified atmospheres with a moderately dense and a thin wind. The need for using unified model atmospheres is clearly visible for the denser wind.

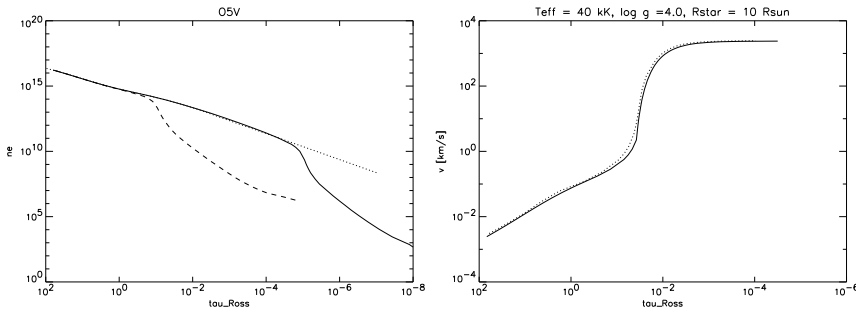


Figure 3: (Left) Electron-density as a function of the Rosseland optical depth,  $\tau_{\text{Ross}}$ , for different atmospheric models of an O5-dwarf. Dotted: hydrostatic model atmosphere; solid, dashed: unified model with a thin and a moderately dense wind, respectively. In case of the denser wind, the cores of optical lines ( $\tau_{\text{Ross}} \approx 10^{-1} - 10^{-2}$ ) are formed at significantly different densities than in the hydrostatic model, whereas the unified, thin-wind model and the hydrostatic one would lead to similar results.

Figure 4: (Right) Velocity fields in unified models of an O-star with a thin wind. Dotted: hydrodynamic solution; solid: analytical velocity law (Eq. 3) with similar terminal velocity and  $\beta = 0.8$  (see text).

By means of a typical velocity law (with  $\beta = 1$ , see Eq. 3), one can calculate the maximum mass-loss rate for which a hydrostatic treatment is still possible, at least for UV and optical lines. From the condition that unified models are required if  $\tau_{\text{Ross}} \geq 10^{-2}$  at the transition between the photosphere and the wind (which is roughly located at 10% of the sound-speed), one finds  $\dot{M} \lesssim 6 \cdot 10^{-8} M_{\odot} \text{yr}^{-1} (R_{*}/10 R_{\odot}) (v_{\infty}/1000 \text{ km s}^{-1})$ . Comparing with “observed” mass-loss rates, this limit implies that hydrostatic models are possible for the UV/optical spectroscopy of late O-dwarfs, B-stars until luminosity class II (for early sub-types) or Ib (for mid/late sub-types), and A-stars until luminosity class Ib. In any case, however, a check is required (if hydrostatic models are used), typically by comparing the observed mass-loss indicator,  $H_{\alpha}$ , with the corresponding synthetic profile. If the observed core of this line is significantly shallower than the synthetic one, wind-effects *do* play a role and unified models have to be used for the analysis. Note that unified model atmospheres are computationally expensive, due to the need of accounting for the velocity-field induced Doppler shifts. Usually, this is done by solving the radiative transfer in the comoving frame (Mihalas et al. 1975, 1976). A faster method bases on the Sobolev approximation (Sobolev 1960) but is justified only for those lines which are formed predominantly in the wind<sup>4</sup>, thus prohibiting the analysis of optical lines under typical conditions (e.g., Santolaya-Rey et al. 1996)

Unified model atmospheres may be constructed in two different ways. First, the complete (wind+photospheric) stratification is derived from a (self-) consistent approach, solving the hydrodynamic equations under the assumption of stationarity. In this case, the equation of momentum has to account for gravity and radiative acceleration (from Thomson-scattering, bound-free transitions, and line-transitions) as external forces, where the radiative acceleration follows from the NLTE-occupation numbers and the radiation field. As shown by CAK, the *line*-acceleration can be represented in the form of Thomson acceleration times a so-called force multiplier. In this description, the total line force as arising from summing up the multitude of individual contributions can be cast into one simple expression, depending on the density, velocity gradient, dilution factor, and three parameters which approximate the statistical distribution of the individual line-strengths. For a self-consistent description of the wind, these parameters have to be obtained from a multi-dimensional regression of the actual line force calculated under NLTE conditions. The force-multiplier approach allows for a rather

<sup>4</sup>more precisely: above the point where the velocity is larger than the thermal/turbulent speed of the considered ion.

easy solution of the stationary wind dynamics, and is used within the model atmosphere code WM-basic (Pauldrach et al. 2001) to set up the density and velocity stratification throughout the complete atmosphere.

The alternative approach is based on an analytical description of the wind. In this case, the density and velocity field are described via

$$\rho(r) = \frac{\dot{M}}{4\pi r^2 v(r)}; \quad v(r) = v_\infty \left(1 - \frac{R_t}{r}\right)^\beta, \quad (3)$$

where mass-loss rate  $\dot{M}$ , terminal velocity  $v_\infty$ , and velocity field parameter  $\beta$  (typically in the range 0.8 - 2) are input and fit parameters. The transition radius,  $R_t$ , has to be calculated from the requirement of a smooth transition between the quasi-hydrostatic photosphere and the wind. As already mentioned,  $R_t$  is located at roughly 10% of the sound speed. The specific form of the analytical velocity law (Eq. 3) is a generalization of hydrodynamic solutions for line-driven winds from stars of different spectral types, and approximates such solutions quite well, as indicated in Fig. 4.

In this approach, the *photospheric* density stratification is calculated as for a hydrostatic atmosphere (but accounting for sphericity), from large optical depths until  $R_t$ , and can be roughly described by an exponential distribution with respect to radius in units of  $H$ . The corresponding velocity law is obtained by using the continuity equation with mass-loss rate from above and photospheric density,  $\rho(r)$ .

#### Unstable stellar winds

From early on (Lucy & Solomon 1970), there was the theoretical prediction that line-driven winds should be affected by a strong instability, inherent to the driving mechanism itself, called the line-driven or de-shadowing instability, thus rendering a stationary description at least questionable. E.g., for short-wavelength perturbations, one obtains  $\delta g_{\text{rad}}^{\text{line}} \propto \delta v$ . First linear analyses (Owocki & Rybicki 1984, 1985) followed by a number of time-dependent hydrodynamical simulations by the groups of S. Owocki and A. Feldmeier confirmed this prediction. Recent results have been published for the 1-D case by Runacres & Owocki (2002, 2005) and for a simplified 2-D description by Dessart & Owocki (2003, 2005). The major result of these investigations - which cannot be *directly* used for model atmosphere calculations, since they are very time-consuming and base on line-statistics rather than individual NLTE-occupation numbers - can be summarized as follows: Beyond a rather stable lower wind, the outer wind ( $r \gtrsim 1.3R_*$ ) develops extensive structure that consists of strong *reverse* shocks separating slower, dense material from high-speed rarefied regions in between. Fortunately, however, the gross quantities, such as  $\dot{M}$  and  $v_\infty$ , but also the density and velocity with respect to the *mass distribution*, are quite similar to the results from a stationary approach. Given the intrinsic mass-weighting of spectral formation, this suggests that at least lines with opacities proportional to the local density (e.g., UV-resonance lines) should be only weakly affected by the time-dependent structure of the wind (e.g., Puls et al. 1993).

In combination with a wealth of independent observational evidence, however, there are at least two principal features of such unstable winds which have to be transferred into the (stationary) atmospheric modeling, in order to allow for a more realistic description of occupation numbers and resulting synthetic SEDs and line profiles.

**X-ray emission of hot stars.** The presence of shocks in time-dependent wind-models (with jump velocities of the order of a few hundred  $\text{km s}^{-1}$ ) lead to the prediction that massive stars should be X-ray emitters, and such X-ray emission has indeed been observed by EINSTEIN, ROSAT, CHANDRA, and XMM-NEWTON. For O-stars, these observations imply  $L_x/L_{\text{bol}} \approx 10^{-7}$ , temperatures of  $T_s \approx 10^6 - 10^7$  K, and volume filling factors,  $f_{\text{vol}}$ , of a few percent.

The conventional way to include this X-ray emission into unified atmospheric models is to assume a two-component wind (e.g., Hillier et al. 1993), with a small fraction (described by the volume filling factor) of shock-heated X-ray emitting gas, where the emission coefficient is described by an appropriate cooling function (depending on shock temperature and density), and a cool, X-ray absorbing wind (with density and velocity as described above). As shown by Pauldrach et al. (1994), the X-ray emission leads to significantly more flux below the He II edge (228 Å) and is an additional source of ionization (directly and via Auger-ionization) for ions of higher stages such as C IV, O IV, O V, O VI, N V, where most of these ions show strong resonance lines in the UV. Only an inclusion of X-rays can, e.g., explain the strong O VI resonance line as observed in most O-supergiants (Pauldrach et al. 1994). If included into the unified models, at least three additional parameters are required,  $L_x$ ,  $T_s$ , and  $f_{vol}$ , where the last two might depend on the distance from the star.

**Wind clumping.** During recent years, there have been various direct and indirect indications that hot star winds are not smooth, but clumpy, i.e., that there are small-scale density inhomogeneities which redistribute the matter into over-dense clumps and an almost void inter-clump medium. Such inhomogeneities are thought to be related to the structure formed in unstable line-driven winds (see above).

When treating wind-clumping in unified atmosphere codes, the standard assumption relates to the presence of optically *thin* clumps and a void inter-clump medium. A consistent treatment of the disturbed velocity field is still missing. The over-density (with respect to the average density) inside the clumps is described by a “clumping factor”,  $f_{cl}$ . The most important consequence of such a structure is that any  $\dot{M}$  derived from standard diagnostics based on processes with  $\rho^2$ -dependent opacities (such as H $\alpha$  or the free-free radio excess) using *homogeneous models* needs to be scaled down by a factor of  $\sqrt{f_{cl}}$ .

Based on this approach, Crowther et al (2002), Hillier et al. 2003, Bouret et al. (2003, 2005) derived clumping factors of the order of 10 - 50, with clumping starting at or close to the wind base (in contradiction to theoretical expectations, but see Cantiello, this volume). From these values, a reduction of previous (unclumped) mass-loss rates by factors of 3 - 7 seems necessary. The *radial* stratification of the clumping factor has been studied by Puls et al. 2006, from a simultaneous modeling of H $\alpha$ , IR, mm and radio observations. They found that, at least in dense winds, clumping is stronger in the lower wind than in the outer part, by factors of 4 - 6, and that unclumped mass-loss rates need to be reduced *at least* by factors 2 - 3.

Even worse, the analysis of the FUV P v-lines by Fullerton (2006) seems to imply mass-loss reductions by factors of 10 or larger, which would have an enormous impact on massive star evolution. However, as suggested by Oskinova (2007), the analysis of such optically *thick* lines might require the consideration of wind “porosity”, which reduces the *effective* opacity at optically thick frequencies (Owocki et al. 2004). Consequently, the reduction of  $\dot{M}$  as implied by the work from Fullerton et al. might be overestimated, and factors similar to those quoted above (around three) are more likely, particularly if considering independent arguments based on stellar evolution, such as the observed ratio of O and WR-stars (see Puls et al. 2008 and references therein).

#### State-of-the-art, NLTE model atmosphere codes

Table 1 enumerates and compares presently available atmospheric codes which can be used for the spectroscopic analysis of hot stars. Since the codes DETAIL/SURFACE and TLUSTY calculate occupation numbers/spectra on top of hydrostatic, plane-parallel atmospheres, they are “only” suited for the analysis of stars with negligible winds (see above). The different computation times are majorly caused by the different approaches to deal with line-blocking/blanketing. The overall agreement between the various codes (within their domain

Table 1: Comparison of state-of-the-art, NLTE, line-blanketed model atmosphere codes.

code	Detail/ surface <sup>1</sup>	TLUSTY <sup>2</sup>	POWR <sup>3</sup>	PHOENIX <sup>4</sup>	CMFGEN <sup>5</sup>	WM-basic <sup>6</sup>	FASTWIND <sup>7</sup>
geometry	plane-parallel	plane-parallel	spherical	spherical/pl.-parallel	spherical	spherical	spherical
blanketing	LTE	yes	yes	yes	yes	yes	approx.
diagnostic range	no limitations	no limitations	no limitations	no limitations	no limitations	UV	optical/IR
major application	BA stars with negl. winds	hot stars with negl. winds	WRs	cool stars, SNe	OB(A)-stars, WRs, SNe	hot stars w. dense winds, SNe	OB-stars, early A-sgs
comments	no wind	no wind	–	no clumping no X-rays	–	no clumping	no X-rays
execution time	few minutes	hours	hours	hours	hours	1 to 2 h	few min. to 0.5 h

(1) Giddings (1981), Butler & Giddings (1985); (2) Hubeny (1998), (3) Gräfener et al. (2002), (4) Hauschildt (1992), (5) Hillier & Miller (1998), (6) Pauldrach et al. (2001), (7) Puls et al. (2005)

of application) is quite satisfactory, though certain discrepancies are found in specific parameter ranges, particularly regarding EUV ionizing fluxes (Puls et al. 2005, Simón-Díaz et al. 2008). Recent results of the application of these codes with respect to the determination of the stellar and wind parameters of massive stars have been summarized by F. Martins (this volume).

## Massive stars, winds and pulsations

In this section, I provide some examples of the potential impact of stellar pulsations on the atmospheres of massive stars.

Stars with a luminosity to mass ratio exceeding  $\sim 10^4 L_{\odot}/M_{\odot}$  should be subject to “strange mode” oscillations (Saio, this volume). Interestingly, optical line profile variability shows the highest amplitudes just in that region of the HRD where strange mode oscillations should be present (Fullerton et al. 1996). Particularly important is the finding that the acoustic energy of such oscillations might be sufficient to initiate the mass-loss of WR-stars (Glatzel, this volume), which to-date is unexplained for a large fraction of these objects.

At least B-supergiants show line profiles which require substantial extra line-broadening (in addition to rotational broadening), denoted by “macro-turbulence” and conventionally described by a supersonic, Gaussian velocity distribution in the photosphere (see K. Uytterhoeven, this volume). As shown by Aerts et al. (this volume), such broadening might be *physically* explained as due to collective effects from low-amplitude, g-mode oscillations. Indeed, the spectroscopic analysis of 29 periodically variable B-supergiants<sup>5</sup> by Lefever et al. (2007), using unified model atmospheres as described above, revealed that most of them are located very close to the high gravity limit of the predicted pre-TAMS instability strip of high order g-modes (SPB-type, Pamyatnykh 1999) and/or within the corresponding post-TAMS instability strip of evolved stars, as predicted by Saio et al. (2006).

Non-radial pulsations (NRPs) might also be responsible for inducing *large-scale* structures in stellar winds, particularly so-called co-rotating interaction regions (Blomme, Lobel, this volume).

Finally, Feldmeier et al. (1997, 1998) showed that the generation of X-rays due to the self-excited line-driven instability alone results in too weak (factor of  $\sim 100$ ) X-ray luminosities. To reproduce the observed values, photospheric disturbances are required to provide deep-seated seeds for clump formation, where subsequent clump-clump collisions are very effective in producing strong X-ray emission *when the photospheric excitation mechanism contains*

<sup>5</sup>detected by Waelkens et al. (1998) from HIPPARCOS data.

a multitude of frequencies. This makes NRPs a prominent candidate for this process.

**Acknowledgments.** J.P. gratefully acknowledges a travel grant by HELAS.

## References

- Anderson, L.S. 1985, ApJ, 298, 848  
 Anderson, L.S. 1989, ApJ, 339, 558  
 Bouret, J.C., Lanz, T., Hillier, D.J., et al. 2003, ApJ, 595, 1182  
 Bouret, J.C., Lanz, T., & Hillier, D.J. 2005, A&A, 438, 301  
 Butler, K., & Giddings J.R. 1985, Newsl. Anal. Astron. Spectra, No. 9  
 Castor, J.I., Abbott, D.C., & Klein R.I. 1975, ApJ, 195, 157 (CAK)  
 Crowther, P.A., Hillier, D.J., Evans, C.J., et al. 2002, ApJ, 579, 774  
 Dessart, L., & Owocki, S.P. 2003, A&A, 406, L1  
 Dessart, L., & Owocki, S.P. 2005, A&A, 437, 657  
 Feldmeier, A., Puls, J., & Pauldrach, A.W.A. 1997, A&A, 322, 878  
 Feldmeier, A., Pauldrach, A.W.A., & Puls, J. 1998, ASP conf. ser., 131, 278  
 Friend, D.B., & Abbott, D.C. 1986, ApJ, 311, 701  
 Fullerton, A.W., Massa, D.L., & Prinja, R.K. 2006, ApJ, 637, 1025  
 Giddings J.R. 1981, Ph.D. thesis, Univ. London  
 Gräfener, G., Koesterke, L., & Hamann, W.-R., A&A, 387, 244  
 Hauschildt, P.H. 1992, J.Q.S.R.T., 47, 433  
 Hillier, D.J., & Miller, D.L. 1998, ApJ, 496, 407  
 Hillier, D.J., Kudritzki, R.-P., Pauldrach, A.W.A., et al. 1993, A&A, 276, 117  
 Hillier, D.J., Lanz, T., Heap, S.R., et al. 2003, ApJ, 588, 1039  
 Hubeny, I. 1998, ASP conf. ser., 138, 139  
 Hummer, D.G., Abbott, D.C., Voels, S.A., & Bohannon, B. 1988, ApJ, 328, 704  
 Hummer, D.G., Berrington, K.A., Eissner, W., et al. 1993, A&A, 279, 298  
 Iglesias, C.A., & Rogers, F.J. 1996, ApJ, 464, 943  
 Kudritzki, R.-P., & Puls, J. 1994, ARA&A, 38, 613  
 Kurucz, R.L. 1979, ApJS, 40, 1  
 Lefever, K., Puls, J., & Aerts, C. 2007 A&A, 463, 1093  
 Lucy, L.B., & Solomon, P.M. 1970, ApJ, 159, 879  
 Mihalas, D., Kunasz, P., & Hummer, D.G. 1975, ApJ, 202, 465  
 Mihalas, D., Kunasz, P., & Hummer, D.G. 1976, ApJ, 206, 515  
 Owocki, S.P., & Rybicki, G.B. 1984, ApJ, 284, 337  
 Owocki, S.P., & Rybicki, G.B. 1985, ApJ, 299, 265  
 Owocki, S.P., Gayley, K.G., & Shaviv, N.J. 2004, ApJ, 616, 525  
 Oskinova, L.M., Hamann, W.-R., & Feldmeier, A. 2007, A&A, 476, 1331  
 Pamyatnykh, A.A. 1999, Acta Astronomica, 49, 119  
 Pauldrach, A.W.A., Puls, J., & Kudritzki, R.-P. 1986, A&A, 164, 86  
 Pauldrach, A.W.A., Kudritzki, R.-P., Puls, J., et al. 1994, A&A, 283, 525  
 Pauldrach, A.W.A., Hoffmann, T.L., & Lennon, M. 2001, A&A, 375, 161  
 Percival, I.C., & Richards, D. 1978, MNRAS, 183, 329  
 Puls, J., Owocki, S.P., & Fullerton, A.W. 1993, A&A, 279, 457  
 Puls, J., Urbaneja, M.A., Venero, R., et al. 2005, A&A, 435, 669



- Puls, J., Markova, N., Scuderi, S., et al. 2006, *A&A*, 454, 625
- Puls, J., Vink, J.S., & Najarro, F. 2008, *AARev*, in press
- Przybilla, N., & Butler, K. 2001, *A&A*, 379, 955
- Przybilla, N., & Butler, K. 2004, *ApJ*, 609, 1181
- Repolust, T., Puls, J., & Herrero, A. 2004, *A&A*, 415, 349
- Runacres, M.C., & Owocki, S.P. 2002, *A&A*, 381, 1015
- Runacres, M.C., & Owocki, S.P. 2005, *A&A*, 429, 323
- Saio, H., Kuschnig, R., Gautschy, A., et al. 2006, *ApJ*, 650, 1111
- Santolaya-Rey, A.E., Puls J., & Herrero A. 1997, *A&A*, 323, 488
- Seaton, M.J., Zeppen, C.J., Tully, J. A., et al. 1992, *Rev. Mex. AA*, 23, 19
- Simón-Díaz, S., & Stasińska, G. 2008, *ArXiv e-prints*, 805, arXiv:0805.1362
- Sobolev, V.V. 1960, "Moving envelopes of stars", Cambridge: Harvard University Press
- van Regemorter, H. 1962, *ApJ*, 136, 906
- Waelkens, C., Aerts, C., Kestens, E., et al. 1998, *A&A*, 330, 215
- Witthoef, M.C., & Badnell, N.R. 2008, *A&A*, 481, 543